Surface Oxygen Vacancy Formation on CeO₂ and its Role in the Oxidation of Carbon Monoxide

Thi X. T. Sayle,[a] Stephen C. Parker[b] and C. Richard A. Catlow*[a]

[a] Davy Faraday Research Laboratory, Royal Institution of Great Britain, 21 Albemarle Street, London W1X 4BS, UK
[b] School of Chemistry, University of Bath, Claverton Down, Bath BA1 7AY, UK

Calculations of defect formation energies at ceria (CeO₂) surfaces using atomistic simulation techniques based on the Born model of the ionic solid predict the enhancement of carbon monoxide oxidation.

The addition of ceria to a ceramic support of alumina and transition metals such as Pt, Pd and Rh has been shown to enhance the effectiveness of the three-way catalyst reactions in automobile exhaust catalysis.[1,2] The importance of this catalyst lies in its ability to convert carbon monoxide, nitrogen oxides and hydrocarbons into non-toxic products. The role of ceria in the exhaust catalyst is complex and not yet well understood. One important aspect is the non-stoichiometry of ceria, which arises from the fact that cerium can readily change its oxidation state. This allows the reversible addition and removal of oxygens, which enables cerium dioxide to act as an oxygen store in oxidation reactions. In this work, we have calculated the energy for carbon monoxide oxidation using oxygen donated from ceria, both from the bulk of the material and from the surface sites.

The simulations were carried out using the energy-minimisation codes CASCADE[3] for the bulk, and MIDAS[4] and CHAOS[5] for the surface simulations. The interionic potentials were based on the Born model of the solid, which includes a long-range coulombic interaction, and a short-range term to model the repulsions and van der Waals attractions between electron charge clouds; the shell model is used to describe the electronic polarisability of the component ions.

The interatomic potential for the O–O interaction was derived empirically by Lewis and Catlow[6] and those for cation–oxygen interactions were calculated using the electron gas method;[7] parameters are reported in Tables 1 and 2. The advantage of using calculated interatomic potentials is that new potentials for impurities can be generated easily. This is particularly important for investigating the effect of the transition metals Pd, Pt and Rh.

The defect energies were simulated using the Mott–Littleton approach (employing the CASCADE code) in which the ions in an inner region around a defect were relaxed explicitly until they experience no net forces, and ions further from the defect were treated using a continuum approach.[8] The same method has been adapted to the study of surface defects (using the CHAOS code).

Table 1 Short range potential parameters

	$V(r) = Ae^{-r/\rho} - C/r^6$		
	A/eV	ρ/Å^{-1}	C/eV Å^{-6}
$O^{2-} - O^{2-}$	22764.3	0.149	43.83
$Ce^{4+} - O^{2-}$	1986.83	0.35107	20.4
$Ce^{3+} - O^{2-}$	1731.61808	0.36372	14.43256

Table 2 Shell model parameters

	$V(r) = k_1 r^2 + k_2 r^4$		
	Y^a(e)	k_1/eV Å^{-2}	k_2/eV Å^{-4}
Ce^{4+}	7.7	291.75	0.0
Ce^{3+}	7.7	291.75	0.0
O^{2-}	-6.1	419.874	10000.0

^{a} Y = shell charge

Cerium dioxide possesses the fluorite structure with each Ce^{4+} surrounded by eight equivalent nearest O^{2-} ions forming the corners of a cube with each O^2-ion being coordinated to four Ce^{4+} ions. We first modelled the two lowest index (111) and (110) surfaces. The (110) surface has stoichiometric proportions of anions and cations in each plane parallel to the surface. The (111) surface comprises a symmetrical stacking sequence of three charged planes; oxygen is at the surface above a plane of cerium ions, which are above a further oxygen plane. This sequence has no dipole moment perpendicular to the surface. The surface energy was then calculated (being defined as the energy per unit area required to form each surface). The resulting energies are given in Table 3.

Two points emerge from these results. First, the surface energies corresponding to the relaxed structures are lower than those for unrelaxed structures; the relaxed energy is 30% lower than the unrelaxed energy for the (111) surface and is 56% for the (110) surface. Secondly, the (111) surface is shown to be more stable than the (110) surface both before and after relaxation. The relaxation of the ions to the equilibrium positions has an important effect on the surface energy. The (110) surface exhibits greater relaxation, which could be due to the high strain on the surface that contains both anions and cations.

The relaxed structures of these two surfaces were then used for the calculations employing CHAOS of the formation energies of isolated defects including the oxygen vacancy and reduction of cerium species. The corresponding calculations were also performed for the bulk crystals using CASCADE. We have then calculated the energies of the reduction for reaction (1) where, by Ce'_{Ce}, we represent the reduction to Ce^{3+}. Results are reported in Table 4.

$$O_O + 2Ce_{Ce} \rightarrow V_{\ddot{O}} + 2Ce'_{Ce} + 1/2\ O_2 \qquad (1)$$
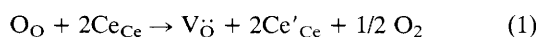
The results indicate three points. First, the energies of the oxygen vacancy and the reduced Ce^{3+} are lower on the surface than in the bulk. Secondly, the energy of reduction for the above reaction [eqn. (6) in Table 4] is more exothermic for both surfaces than for the bulk, suggesting that it is easier to abstract oxygen from the surface. In addition, the energy of the reduction on the (110) surface is more exothermic owing to the lower oxygen vacancy formation energy [eqn. (3)] and lower reduction energy [eqn. (1)]. This behaviour may be because the (110) surface is less stable and hence more active. While no direct comparison can be made with the measured energies, a value of 4.77 eV for the relative partial molar enthalpy of oxygen per atom at 1353 K for CeO_2 was reported;[9] inclusion of clustering might be expected to bring the calculated value of 6.58 eV into closer agreement.

The most important single result of this study is the demonstration that the oxidation of carbon monoxide using oxygen from CeO_2 is favourable at the less stable (110) surface

Table 3 Surface energies of the two most stable surfaces of CeO_2

Surface	Surface energy/J m^{-2}	
	Before relaxation	After relaxation
(111)	1.707	1.195
(110)	3.597	1.575

Table 4 Defect equilibria for the carbon monoxide oxidation in ceria support

		Energy/eV		
			Surface	
	Defect equilibria	Bulk	(111)	(110)
(1)^a	$2\,Ce^{4+}_L \rightarrow 2\,Ce^{3+}_L$	73.91	70.45	68.36
(2)^b	$2\,e^-_\infty + 2\,Ce^{4+}_\infty \rightarrow 2\,Ce^{3+}_\infty$	-73.52	-73.52	-73.52
(3)^c	$O^{2-}_L \rightarrow O^{2-}_\infty + V_{\ddot{O}}$	16.06	15.65	14.56
(4)^d	$O^{2-}_\infty \rightarrow O_\infty$	-7.29	-7.29	-7.29
(5)^e	$O_\infty \rightarrow 1/2\,O_2$	-2.58	-2.58	-2.58
(6)^f	$O_O + 2\,Ce_{Ce} \rightarrow$ $V_{\ddot{O}} + 2\,Ce'_{Ce} + 1/2\,O_2$	6.58	2.71	-0.47
(7)^g	$CO_{(g)} + 1/2\,O_{2(g)} \rightarrow CO_{2(g)}$	-2.93	-2.93	-2.93
(8)^h	$CO_{(g)} + O_O + 2\,Ce_{Ce} \rightarrow$ $V_{\ddot{O}} + 2\,Ce'_{Ce} + CO_{2(g)}$	3.65	-0.22	-3.40

^{a} Substitution energy of Ce^{4+} for Ce^{3+} in the lattice. ^{b} The fourth ionization energy of cerium.[10] ^{c} Oxygen vacancy formation. ^{d} 1st and 2nd electron affinity of oxygen.[11] ^{e} Bond dissociation of oxygen.[10] ^{f} Formation of molecular oxygen from cerium oxide. ^{g} Enthalpy of carbon monoxide oxidation.[10] ^{h} Overall reaction.

owing to its high exothermic energy; the enthalpy for the reaction at the (111) surface is less exothermic and that for the bulk is very endothermic indicating an unfavourable reaction. Thus, we predict that any processing conditions that favour the formation of the (110) surface will show this enhanced activity towards oxidation.

In summary, we have illustrated that by using an accurate potential model together with modern computational techniques, we can study the factors that govern the reactivity of solid oxide surfaces.

References

1 H. C. Yao and Y. Yu Yao, *J. Catal.*, 1984, **86**, 254.
2 M. G. Sanchez and J. L. Gazquez, *J. Catal.*, 1987, **104**, 120.
3 M. Leslie, SERC Daresbury laboratory report DL/SCI/TM31T.
4 J. H. Harding, AERE R 14300, Theoretical Physics Division, AERE Harwell, Oxfordshire, UK.
5 D. M. Duffy and P. W. Tasker, AERE R 11059, see ref. 4 for address.
6 G. V. Lewis and C. R. A. Catlow, *J. Phys. C: Sol. State Phys.*, 1985, **18**, 1149.
7 J. H. Harding and A. H. Harker, AERE R 10425, see ref. 4 for address.
8 C. R. A. Catlow and W. C. Mackrodt, *Computer Simulation of Solids Lecture Notes in Physics*, vol. 166, Springer, Berlin, 1982.
9 R. Tetot, C. Picard, G. Boureau, P. Gerdanian, *Advances in Ceramics*, ed. C. R. A. Catlow and W. C. Mackrodt, 1987, **23**, 457.
10 W. East, *Handbook of Chemistry and Physics*, 1971.
11 G. W. C. Kaye and T. H. Laby, *Tables of Physical and Chemical Constants*, 1966.